Since January 2020 Elsevier has created a COVID-19 resource centre with free information in English and Mandarin on the novel coronavirus COVID-19. The COVID-19 resource centre is hosted on Elsevier Connect, the company's public news and information website.

Journal of Immunological Methods 373 (2011) 89–101

Contents lists available at SciVerse ScienceDirect

Journal of Immunological Methods

journal homepage: www.elsevier.com/locate/jim

Research paper

MAp19, the alternative splice product of the *MASP2* gene

Søren E. Degn [a,*], Steffen Thiel [a], Ole Nielsen [b], Annette G. Hansen [a], Rudi Steffensen [c], Jens C. Jensenius [a]

[a] Department of Biomedicine, Aarhus University, Wilhelm Meyers Allé 4, DK-8000 Aarhus C, Denmark
[b] Department of Clinical Pathology, Odense University Hospital, Winsløwparken 15, 5000 Odense C, Denmark
[c] Regional Centre for Blood Transfusion and Clinical Immunology, Aalborg Hospital, Urbansgade 36, DK-9000 Aalborg, Denmark

ARTICLE INFO

Article history:
Received 27 May 2011
Received in revised form 19 July 2011
Accepted 8 August 2011
Available online 17 August 2011

Keywords:
Complement
Lectin pathway
Mannan-binding lectin
MAp19
sMAP
MASP-2

ABSTRACT

The lectin pathway of complement is a central part of innate immunity, but as a powerful inducer of inflammation it needs to be tightly controlled. The *MASP2* gene encodes two proteins, MASP-2 and MAp19. MASP-2 is the serine protease responsible for lectin pathway activation. The smaller alternative splice product, MAp19, lacks a catalytic domain but retains two of three domains involved in association with the pattern-recognition molecules (PRMs): mannan-binding lectin (MBL), H-ficolin, L-ficolin and M-ficolin. MAp19 reportedly acts as a competitive inhibitor of MASP-2-mediated complement activation. In light of a ten times lower affinity of MAp19, versus MASP-2, for association with the PRMs, much higher serum concentrations of MAp19 than MASP-2 would be required for MAp19 to exert such an inhibitory activity. Just four amino acid residues distinguish MAp19 from MASP-2, and these are conserved between man, mouse and rat. Nonetheless we generated monoclonal rat anti-MAp19 antibodies and established a quantitative assay. We found the concentration of MAp19 in serum to be 217 ng/ml, i.e., 11 nM, comparable to the 7 nM of MASP-2. In serum all MASP-2, but only a minor fraction of MAp19, was associated with PRMs. In contrast to previous reports we found that MAp19 could not compete with MASP-2 for binding to MBL, nor could it inhibit MASP-2-mediated complement activation. Immunohistochemical analyses combined with qRT-PCR revealed that both MAp19 and MASP-2 were mainly expressed in hepatocytes. High levels of MAp19 were found in urine, where MASP-2 was absent.

1. Introduction

The recognition of non-self by the innate immune system is mediated by cellular and humoral pattern-recognition molecules (PRMs), targeting conserved pathogen-associated molecular patterns (PAMPs). A group of humoral PRMs, mannan-binding lectin (MBL), H-ficolin, L-ficolin, and M-ficolin, can activate the lectin pathway of complement by means of associated serine proteases, MASP-1, MASP-2 and MASP-3 (Thiel, 2007). Two additional proteins, MAp19 and MAp44, are found associated with these PRMs.

MAp19, also known as sMAP, is one of two proteins arising by alternative splicing of the primary transcript of the *MASP-2* gene (Stover et al., 1999b; Takahashi et al., 1999). The other product is the pro-enzyme MASP-2, which is composed of a CUB domain, an EGF domain, a second CUB domain, two CCP domains and the activation peptide, followed by the serine protease domain (Thiel et al., 1997). Mature MASP-2 is generated by cleavage of the activation peptide, resulting in two disulfide-linked fragments, the larger known as the A-

Abbreviations: MBL, mannan-binding lectin;MASP, MBL-associated serine protease;MAp, MBL-associated protein;pAb, polyclonal antibody;MBS, m-maleimidobenzoyl-N-hydroxysuccinimid;DVS, divinylsulfone;PPD, purified protein derivative;HRP, horseradish peroxidase;KLH, keyhole limpet hemocyanin;BCG, Bacillus Calmette-Guérin;C1-Inh, C1 inhibitor;o.n., overnight;pMBL/MASP, plasma-derived MBL/MASP complexes;PAMP, pathogen-associated molecular pattern;PRM, pattern-recognition molecule;hIgG, normal human IgG;NHS, normal human serum;TRIFMA, time-resolved immunofluorometric assay;RT, room temperature.

* Corresponding author. Tel.: +45 89 42 17 78; fax: +45 86 19 61 28.
E-mail address: sdegn@microbiology.au.dk (S.E. Degn).

0022-1759/$ – see front matter © 2011 Elsevier B.V. All rights reserved.
doi:10.1016/j.jim.2011.08.006

chain and the smaller as the B-chain (Schwaeble et al., 2002; Thiel, 2007). MAp19 consists of only the first CUB domain and the EGF domain, with an additional small C-terminal tail of four unique amino acid residues (EQSL) (Fig. 1). These four amino acid residues are encoded by exon 5 of the gene, which also harbors the 3′UTR. Like MASP-2, MAp19 is known to be expressed in the liver and is found in plasma (Stover et al., 1999a). It forms a head-to-tail dimer, the structure of which has been solved by X-ray crystallography to a resolution of 2.5 Å (Gregory et al., 2004), and associates with MBL and the ficolins in a calcium-dependent manner. The dissociation constant for the interaction with MBL has been determined to be 13 nM, identical to the similar CUB-EGF fragment of MASP-2, but around 16 times higher than that of full-length MASP-2 (Thielens et al., 2001). MAp19 has been suggested to act as an inhibitor of calcium oxalate crystal growth in human urine (Kang et al., 1999). More recently, MAp19 has been reported to compete with MASP-2 for binding to MBL, leading to attenuation of C4-cleaving activity and thus down-regulation of complement activation (Iwaki et al., 2006). MAp19 is relatively well conserved, the amino acid sequence for human MAp19 being 80% and 77% identical with mouse and rat MAp19, respectively, and the unique 4 C-terminal amino acids are conserved between these species (Fig. 1A).

We present the generation of monoclonal antibodies specific for MAp19 and the construction of a solid-phase assay for quantification of MAp19 under dissociating conditions. Using this assay we determine the mean concentration of MAp19 in blood and urine. We compare the mRNA expression profiles of MAp19 and MASP-2, as well as the tissue distribution of the proteins by immunohistochemical analyses. Finally, we characterize the interaction of MAp19 with MBL and ficolins under native conditions and examine the reported inhibitory activity of MAp19 on activation of the complement system.

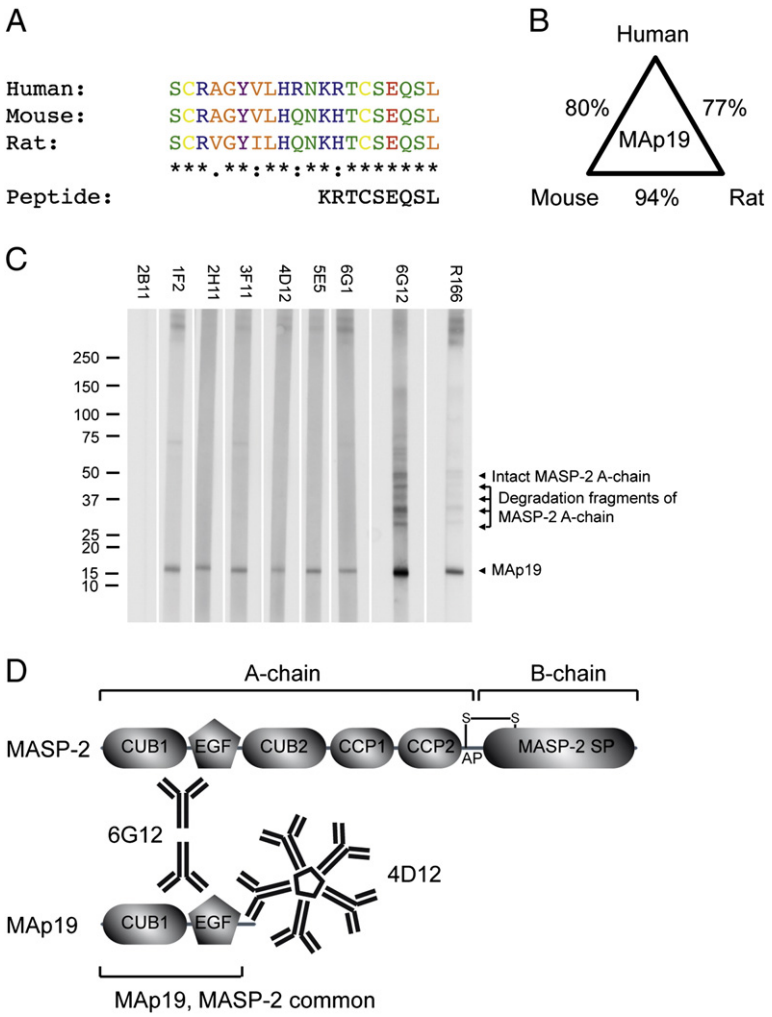

Fig. 1. MAp19 and anti-MAp19 antibodies. A) Alignment of the C-terminal ends of human, mouse and rat MAp19, demonstrating a high degree of conservation with total identity of the 4 ultimate amino acids. The peptide used for immunizations is shown. B) Percent identity between full-length human, mouse and rat MAp19. C) Western blot reactivity of anti-MAp19 antibodies, demonstrating specificity for MAp19. Strips of a Western blot containing purified MBL/MASP complexes from human plasma were developed using hybridoma supernatants as primary antibodies. Negative control is a non-reactive hybridoma (2B11) and positive control is a monoclonal antibody toward MASP-2 and MAp19 (6G12). The parental rat serum (R166) is included, showing similar reactivity to that of the hybridoma supernatants. D) Overview of the domain structure of MAp19 and MASP-2, with indication of approximate antibody epitopes.

2. Materials and methods

2.1. Miscellaneous proteins and antibodies

Recombinant MBL (rMBL), with complement activation capacity similar to that of MBL purified from plasma, was produced as described (Jensenius et al., 2003). Plasmid encoding MASP-3 has been described (Dahl et al., 2001). A pFastBac plasmid encoding human MAp19 cDNA (Thielens et al., 2001) was kindly provided by Nicole Thielens. The insert was excised from the pFastBac vector using BamHI and HindIII and ligated into the pcDNA3.1(−) vector (Invitrogen) for expression in mammalian cells. Resulting colonies were screened by restriction analysis and confirmed by sequencing.

Recombinant MASP-3 and MAp19 were produced by transient expression in FreeStyle HEK293F cells in FreeStyle Expression Medium (Invitrogen). The plasmids were introduced using a cationic lipid-based transfection reagent (Lipofectamine2000, Invitrogen). Following a procedure we have previously described for the purification of rMAp44 (Degn et al., 2009), the rMASP-3 and rMAp19 were purified from the culture supernatants by affinity chromatography on rMBL-coupled Sepharose 4B in a Ca^{2+}-containing buffer, and bound rMASP-3 or rMAp19 was eluted with a buffer containing EDTA and high salt concentration. The purity of the products was verified by silver staining of SDS-PAGE gels. The concentrations of the proteins in the eluates were determined by OD280 measurement (using molar extinction coefficients of 1.02 and 1.22 $(mg/ml)^{-1}$ cm^{-1} for MAp44 and MAp19, respectively, calculated from the sequences using Protein Calculator v.3.3) and confirmed by quantitative amino acid analysis.

MBL/MASP complexes were purified from a pool of human plasma by affinity chromatography on mannan coupled to Sepharose beads, as previously described (Matsushita et al., 2000).

Two monoclonal rat antibodies, 6G12 (isotype IgG1), reacting with the common part of human MAp19 and MASP-2 (Fig. 1D), and 8B5 (IgG1), specific for MASP-2, were previously generated (Møller-Kristensen et al., 2003). Likewise, a mouse monoclonal antibody, 1.3B7 (IgG1κ), reacting with MASP-2 and MAp19 was previously generated (Thiel et al., 2000).

2.2. Generation of MAp19-specific antibodies

A nonapeptide representing the C-terminus of MAp19 (KRTCSEQSL) was synthesized, thus including the four unique C-terminal amino acids of MAp19 and a convenient internal cysteine for coupling. The peptide was coupled to keyhole limpet hemocyanin (KLH) using m-maleimidobenzoyl-N-hydroxysuccinimidyl ester (MBS) and 3 BALB/c mice and 3 Wistar rats were subjected to an immunization regimen with the conjugated peptide in Freund's adjuvant. Sera were screened as indicated below. The mice failed to respond, whereas the rats mounted very limited responses. These 3 rats and further 3 naive rats and 3 naive mice were then subjected to an immunization regiment with peptide coupled to purified protein derivative (PPD) from *Bacillus tuberculosis*. The rats already having received Freund's complete adjuvant were not primed further, whereas the naive animals were primed with 100 µl of BCG vaccine, s.c. in the neck (1.7 adult human doses of *Mycobacterium bovis* Bacillus Calmette-Guérin, an attenuated live vaccine, Statens Serum Institut, Copenhagen).

The PPD-conjugated peptide was produced by three methods: sulfo-MBS coupling, glutaraldehyde coupling and divinylsulfone (DVS) coupling, using about 14-fold molar excess of peptide to PPD. Briefly, for sulfo-MBS coupling, 300 µl of 1 mg PPD/ml was mixed with 300 µl of 1 mg sulfo-MBS/ml 25 mM phosphate buffer, pH 7.2, and incubated for 30 min end over end at room-temperature (RT). Following this, the mixture was dialysed against 25 mM phosphate buffer, pH 7.2, mixed with 600 µl peptide (1 mg/ml 25 mM phosphate buffer, pH 7.2) for 3 h end over end at RT, and then dialysed extensively against PBS (137 mM NaCl, 2.7 mM KCl, 1.5 mM KH_2PO_4, 8.1 mM Na_2HPO_4, pH 7.4). For glutaraldehyde coupling, 300 µl of 1 mg PPD/ml were added to 600 µl of 1 mg peptide/ml 25 mM phosphate buffer, pH 7.2. One ml of 0.12% glutaraldehyde in phosphate buffer was added, followed by incubation for 2 days, end over end at 4 °C, and dialysis against PBS. For DVS coupling, 300 µl of 1 mg PPD/ml was dialyzed against 100 mM carbonate buffer, pH 9.0 and 2.5% (v/v) DVS added, followed by incubation at 4 °C overnight (o.n.) To this mixture was added 300 µl of 1 mg peptide/ml 100 mM carbonate buffer, pH 9.0, followed by incubation o.n., end over end at 4 °C. Finally this was also dialyzed extensively against PBS.

The three coupling reaction products were mixed in approximately equal volume and 150 µl (emulsified 6:9 in Freund's incomplete adjuvant) was used for each immunization. After three rounds of immunizations the rats were still the best responders, and the highest response was generated in a rat previously subjected to the peptide-KLH protocol. This rat was given recombinant MAp19 (rMAp19, see below), i.v., before the spleen was harvested and the cells fused with X63Ag8.653 murine myeloma cells, according to standard protocols (Kohler and Milstein, 1975; Kearney et al., 1979). Resulting aminopterin resistant clones were screened as described below, and subcloned a total of 4 times to ensure monoclonality.

2.3. Screening assays for serum anti-MAp19 antibodies

Sera from immunized animals were screened in several assays, with all reagents added at 100 µl/well:

1) On MBL complexes captured on a mannan coat and on ficolin complexes captured on a coat of acetylated bovine serum albumin (AcBSA). Mannan (polysaccharide from yeast and a strong ligand for MBL, purified according to (Nakajima and Ballou, 1974)) or AcBSA (from Sigma, presenting ligands for all three ficolins (Krarup et al., 2004; Frederiksen et al., 2005)) was coated in microtiter wells (FluoroNunc, Nunc, Denmark) at 10 µg/ml carbonate buffer, pH 9.6, o.n. at 4 °C. Residual binding sites were blocked with 1 mg human serum albumin (HSA, Statens Serum Institut) per ml TBS (10 mM Tris–HCl, 140 mM NaCl, 15 mM NaN_3, pH 7.4), and the wells were washed thrice with TBS containing 5 mM $CaCl_2$ and 0.05% (v/v) Tween-20 (TBS/Tw/Ca^{2+}). A human serum pool diluted 20-fold in binding buffer (20 mM Tris, 1 M NaCl, 10 mM $CaCl_2$, 1 mg HSA/ml, 0.05% (v/v) Triton X-100, pH 7.4) was incubated in the wells at 4 °C o.n. After washing with TBS/Tw/Ca^{2+}, animal sera were added in a 10-fold dilution series in TBS/Tw/Ca^{2+}, from 1/100 to 1/10,000,

and incubated o.n. at 4 °C. Wells were washed with TBS/Tw/Ca^{2+} and developed with biotinylated rabbit-anti-rat Ig or biotinylated rabbit-anti-mouse Ig (both antibodies from DAKO, Z0494 and Z0259, respectively, and biotinylated in-house), followed by Eu^{3+}-streptavidin (PerkinElmer) at 0.1 μg/ml TBS/Tw (TBS with 0.05% Tween-20), containing 25 μM EDTA and incubated for 45 min before final wash and development with enhancement buffer (PerkinElmer) and reading on a time-resolved fluorometer (Victor3, PerkinElmer). The readings are given as photon counts per second. The procedure is termed "time-resolved immunofluorometric assay", abbreviated TRIFMA. As a control for direct reactivity with the surfaces, animal sera were tested on the same primary coats not subjected to incubation with human serum.

2) On directly coated MBL complexes or on H-ficolin complexes, purified from human plasma on mannose-TSK-75 beads and acetylated-HSA-derivatized Sepharose-4B beads, respectively. Plasma-derived MBL/MASP or H-ficolin/MASP complexes were coated in microtiter wells at 1 μg MBL or H-ficolin per ml. Animal sera were added in dilution series as above, and development was performed in a similar manner. A mock-coated surface was used for background control.
3) On wells directly coated with recombinant MAp19, using an approach similar to the one employed for hybridoma supernatants as described below.

2.4. Screening assay for anti-MAp19 antibodies in hybridoma supernatants

Hybridoma supernatants were screened on wells directly coated with rMAp19. rMAp19 was coated in microtiter wells at 0.5 μg/ml PBS o.n. at 4 °C. Wells were blocked with TBS/Tw, washed thrice with TBS/Tw/Ca^{2+}, and hybridoma supernatants diluted 1:1 in TBS/Tw/Ca^{2+} were added. After incubation and washing with TBS/Tw/Ca^{2+}, biotinylated rabbit-anti-rat Ig was added. After incubation the wells were washed with TBS/Tw/Ca^{2+} and developed with Eu^{3+}-streptavidin as described above.

Positive supernatants were further tested in a similar assay based on coating the wells with rMASP-2 (1 μg/ml) in order to ensure lack of cross-reactivity with MASP-2.

2.5. Western blotting

Supernatants tested positive in the MAp19 assay were tested on a Western blot (WB) of plasma-derived MBL/MASP complexes. Forty μl pMBL/MASP preparation (containing 65 μg MBL/ml) was added sample buffer containing DTT and loaded on a single-well XT-Criterion 4–12% gel (Bio-Rad). The proteins were blotted to Hybond-P PVDF membrane (Amersham Biosciences) and strips 0.25 cm wide were cut. Strips were incubated with hybridoma supernatants diluted 1/10 in primary buffer (TBS/Tw, 1 mM EDTA, with 1 mg HSA and 100 μg normal human IgG (hIgG) added per ml), or with the parental rat serum 1/500. After washing 3× with TBS/Tw, without azide, these strips were incubated with horseradish peroxidase (HRP)-conjugated rabbit-anti-rat Ig (P0450, DAKO) diluted 1/1,000 in secondary buffer (TBS/Tw without azide, 1 mM EDTA, 100 μg hIgG/ml). This was followed by washing and development with West Dura extended duration substrate (Pierce). Images were taken using a CCD camera (LAS-3000, Fuji) and analyzed with the software supplied with the camera. As a control, a strip was incubated with a monoclonal rat anti-human MAp19/MASP-2 (6G12, see below) at 1 μg/ml primary buffer, followed by HRP-conjugated rabbit-anti-mouse Ig (P0260, DAKO).

2.6. Determination of antibody isotypes

Recombinant MAp19 was coated at 0.25 μg/ml PBS, o.n. at 4 °C. The wells were blocked with TBS/Tw, and then washed thrice in TBS/Tw. Hybridoma supernatants, diluted 1:1 in TBS/Tw, were added to each well and incubated for 2 h. The wells were washed thrice with TBS/Tw, before the addition of 100 μl affinity-purified and biotinylated anti-rat immunoglobulin class and subclass antibodies (anti-IgG1, -IgG2a, -IgG2b, -IgG2c, -IgA, and -IgM, as well as a control biotinylated normal Ig; Zymed Laboratories, Rat MonoAB ID/SP KIT) in PBS/Tw. Two hours of incubation was followed by washing thrice with TBS/Tw, the addition of Eu^{3+}-streptavidin, and development as described above. In a similar set-up, the anti-MAp19 antibody isotypes present in the parental rat serum was determined (serum diluted 1/10).

2.7. Purification of monoclonal anti-MAp19 antibodies

The anti-MAp19 antibodies were purified on Protein L agarose (Sigma). Approximately 1.5 ml Protein L agarose was pre-washed in 0.1 M glycine, pH 2.5, then equilibrated in PBS and packed in a Poly-Prep Chromatography Column (Bio-Rad). Ninety ml hybridoma supernatant was pre-cleared by centrifugation at 2,000 *g* for 10 min, added 10 ml of 10 times concentrated PBS, and loaded on the column. The effluent was collected in fractions of 10 ml. The column was washed with 15 ml (10 column volumes) PBS and elution was performed with 0.1 M glycine, pH 2.5. The eluate was collected in approximately 10 fractions of 500 μl, into 42 μl 1 M Tris–HCl, pH 8.5, for immediate neutralization. The protein content of the eluates was assessed by OD280 measurement, and protein-containing fractions were pooled. The anti-MAp19 content of the eluates, the pooled eluates and the effluent fractions was assessed by testing on directly coated recombinant MAp19, as described above.

2.8. Test of autoreactivity of the 5 final antibodies and parental rat serum

MBL/MASP and Ficolin/MASP complexes were purified in parallel from human and rat serum. A 1:1 mixture of mannan-coupled sepharose and acetylated HSA-coupled sepharose was washed twice with 25 ml TBS/Tw/0.5 M NaCl/10 mM EDTA, then equilibrated with 4×25 ml TBS/Tw/5 mM $CaCl_2$. To 2.5 ml of this mixture (approximately 2 ml beads) was added either 5 ml normal human serum or 5 ml normal rat serum pre-diluted with 10 ml TBS/Tw/Ca^{2+}. The beads were incubated with the serum samples 1 h end over end at 4 °C, then spun down 5 min at 100 g and washed 3× with 50 ml TBS/Tw/Ca^{2+}. The beads were then packed in Poly-Prep Chromatography Columns and washed with an additional 25 ml TBS/Tw/Ca^{2+}. The column was eluted with TBS/Tw/0.5 M NaCl/10 mM EDTA and fractions of 250 μl

were collected. The OD280 of fractions was measured compared to the elution buffer and peak fractions were pooled. From approximately 1 ml pooled eluates of each, 500 µl was run on a reducing gel, as described above. Proteins were blotted to nitrocellulose, the membranes were blocked with TBS/0.1% Tween and cut into strips, which were then probed with the parental rat serum diluted 1/1,000, and the 5 final clones purified on Protein L agarose diluted to 1 µg/ml, as well as a normal rat serum diluted 1/1,000, all in TBS/Tw/1 mM EDTA/1 mg HSA per ml and 100 µg nhIg per ml. A buffer only control was also included, and for the human blot, an anti MBL antibody (131–1 mouse mAb) was included at 1 µg/ml along with a normal mouse serum control, 1/1,000, in order to confirm presence of MBL in the purified pool. Rat antibodies were developed with HRP-rabbit-anti-rat (DAKO P0450) and mouse antibodies with HRP-rabbit-anti-mouse (DAKO P0260), both diluted 1/3,000 in TBS/Tw/1 mM EDTA/100 µg/ml nhIg.

2.9. MAp19 TRIFMA

A sandwich assay based on the TRIFMA principle was developed, involving capture with mAb 6G12 and detection of bound MAp19 with biotinylated anti-MAp19 antibody (4D12) (Fig. 1) followed by Eu^{3+}-labeled streptavidin. Wells were coated with 4 µg 6 G12 per ml sodium acetate buffer (50 mM Na-acetate, 145 mM NaCl, pH 4.5) o.n. at 4 °C. The wells were then blocked with HSA, 1 mg/ml TBS, washed thrice with TBS/Tw, and incubated with serum samples diluted 20-fold in MAp19 buffer (TBS/Tw, 1 M total NaCl, 10 mM EDTA, containing 100 µg ΔhIgG (heat-aggregated hIgG); Beriglobin, from ZLB Behring GmbH, incubated 30 min at 63 °C and centrifuged 10 min at 3,000 *g* to remove large aggregates) per ml, and 100 µg normal rat IgG (Lampire) per ml) o.n. at RT. The ΔnhIg was added to adsorb any rheumatic factor present in the sample, while the normal rat IgG was added to prevent cross-linking of the coating and the detecting rat antibodies by any anti-rat antibodies in the serum samples (Degn et al., 2011). After washing the wells, biotinylated 4D12 was added at 1 µg per ml TBS/Tw containing 1 mg HSA/ml. Following another wash, the wells were developed with Eu^{3+}-streptavidin as described above. A standard curve was prepared by applying a 2-fold serial dilution of a standard serum (8 dilutions) and a buffer control. Along with three internal control sera (high, medium, low), this was included on every plate. All samples, standards and controls were in duplicates.

Sepharose beads coupled with 6G12 (anti-MAp19/MASP-2), 400 µl (approximately 200 µl bead volume) were washed thrice with 1 ml 0.1 M glycine, pH 2.5, then equilibrated with 10 ml incubation buffer (TBS/Tw, 1 M total NaCl, 10 mM EDTA, containing 100 µg ΔhIgG). The equilibrated beads were incubated with 1 ml of a serum found to be low in MAp19 and MASP-2 and pre-diluted with 3 ml of incubation buffer, for 2 h at RT end over end. The beads were spun down and the supernatant (depleted serum diluted 1/4) was saved. Dilution curves were prepared using the standard serum, the low serum, the low serum depleted of MAp19/MASP-2, the low serum depleted and reconstituted with recombinant MAp19, or recombinant MAp19 diluted in buffer only.

Capacity and specificity tests were carried out by measurement of dilution series of rMAp19 or rMASP-2 prepared in serum diluted 1/20.

2.10. Blood samples and 24 h urine samples

Serum and plasma samples were obtained from a cohort of adult Danish blood donors after informed consent and according to the Declaration of Helsinki. The levels of MBL and MASP-2 (Ytting et al., 2007) and MAp44 and MASP-3 (Degn et al., 2010) were previously determined in these samples. Similarly, paired blood samples and 24 h urine samples were obtained from 5 Danish volunteers. Samples were stored at −80 °C and freeze–thaw cycles were kept to a minimum.

2.11. MAp19 in urine

Urine samples were analyzed by TRIFMA and by Western blotting as described above. Western blots of reduced samples were developed with 4D12, non-reduced samples with 1.3B7.

2.12. Tissue mRNA expression profile of MAp19 and MASP-2

MAp19 and MASP-2 mRNA expression levels were quantified in a FirstChoice Human Total RNA Survey Panel (Applied Biosystems/Ambion) comprising RNA from 20 human tissues, using TaqMan chemistry and the ABI Prism 7000 Sequence Detection System. The RNA was reverse transcribed using the Roche One Step RT-PCR system with oligo(dT) primers. TaqMan gene expression assays from Applied Biosystems were used for MASP-2 (catalog no. Hs00198244_m1) and MAp19 (custom assay targeting exon 4–5), using β_2-microglobulin mRNA (Hs99999907_m1) for normalization. The relative levels of MASP-2 and MAp19 mRNA were compared using the delta–delta cycle threshold method.

2.13. Immunohistochemical analysis of the tissue distribution of MAp19 and MASP-2

Immunohistochemical analysis was performed on formalin-fixed paraffin-embedded tissue multiblocks and similarly prepared multiblocks of HEK293F cells transfected with MAp19 plasmid, MASP-2 plasmid, or mock transfected. Briefly, HEK293F cells were transfected as described above, pelleted 72 h post-transfection, fixed o.n. in 10% neutral-buffered formalin, then subjected to standard protocols for dehydration, clearing and paraffin embedding.

The 3B11 hybridoma supernatant was used to stain for MAp19, at a dilution of 1/300, while the purified monoclonal antibody 8B5 was used to stain for MASP-2, at a dilution of 1/1,000. Endogenous peroxide was blocked by pre-treatment with 1.5% hydrogen peroxide in TBS for 10 min. Antigen retrieval was done by demasking with 15 minute microwave treatment in EGTA-containing Tris buffer. Primary antibodies were diluted in antibody diluent (S2022, DAKO) and incubated on slides for 60 min at RT. The secondary antibody was biotinylated polyclonal rabbit anti-rat Ig (E0468, DAKO; pre-adsorbed to remove any cross-reactivity toward human or mouse immunoglobulins and fetal calf serum) diluted 100-fold in S2022. The procedure was carried out in an AutostainerPlus, using PowerVision + HRP

(mono/poly) (Leica Biosystems) as detection system, and development was performed using the chromogen DAB (K3468, DAKO) for 10 min. Nuclear counterstain was performed using Mayer's heamatoxylin for 2 min, before mounting slides for microscopy using AquaTex (Merck).

2.14. GPC analysis of MAp19 size distribution in human serum

Normal human serum (NHS) was subjected to gel permeation chromatography (GPC) on a Superose 6 column in either TBS with 5 mM $CaCl_2$ or TBS with 850 mM NaCl and 10 mM EDTA (a buffer dissociating the MBL/MASP complexes) (Møller-Kristensen et al., 2003). MAp19 was quantified in the fractions with the assay described above. Fractions were also analyzed for IgM, MBL and H-, L- and M-ficolin. The elution volume of purified IgG and HSA was also determined.

2.15. Test of inhibition of C4 deposition by MAp19 and MAp44

Two-fold dilution series of rMA19 or rMAp44 ranging from 1 μg/ml to 10 ng/ml (corresponding to around 50–0.5 nM) were pre-incubated with a constant amount of rMBL (25 ng/ml) for 15 min at RT. The mixtures were then incubated with 5 ng/ml rMASP-2 for 15 min at RT, before being added to microtiter wells coated with 10 μg mannan per ml, as described above. After incubation at 4 °C o.n. and washing thrice with TBS/Tw/Ca^{2+}, the wells were incubated with 0.1 μg purified human complement component 4 (Dodds, 1993) in 100 μl BBS^{2+} (4 mM barbital, 145 mM NaCl, 2 mM $CaCl_2$, 1 mM $MgCl_2$, 3.8 mM NaN_3, pH 7.5) at 37 °C for 90 min. The wells were then washed and a mixture of two biotin-labeled monoclonal anti-human C4 antibodies (mAb 162.2 and mAb 162.1, both from Bioporto, 0.25 μg of each per ml TBS/Tw/Ca^{2+}) was incubated for 2 h at RT followed by europium-labeled streptavidin and development as described above (Petersen et al., 2001).

To examine whether the competitors affected the binding of MBL to the surface, in a parallel experiment biotin-labeled monoclonal antibody against MBL (131–1) was deployed, and the wells were developed with europium-labeled streptavidin as described above.

3. Results

3.1. Generation, characterization, and validation of MAp19-specific antibodies

MAp19 is highly conserved across species and harbors only 4 C-terminal amino acids distinguishing it from MASP-2 (Fig. 1A and B). Especially the C-terminal part is very well conserved, with no difference in the unique 4 residues between human, mouse and rat. Nonetheless, we designed a peptide (Fig. 1A) encompassing the 4 unique amino acids and conjugated it to KLH or PPD (a heterogeneous protein preparation from *Mycobacterium tuberculosis* acting as a carrier and a potent activator of the adaptive immune system), and immunized BALB/c mice and Wistar rats. Sera were initially unsuccessfully screened in solid-phase assays on MBL/MASP complexes captured on a mannan surface and ficolin/MASP complexes captured on an AcBSA surface. However, we found that we could get signals when screening on purified MBL/MASP/MAp complex or H-ficolin/MASP/MAp complex coated directly onto wells, as well as on directly coated purified recombinant MAp19. The best responder, a Wistar rat, was boosted with rMAp19 before performing the splenectomy and myeloma fusion. The resulting hybridomas were screened in solid-phase assays as before and subcloned. The final hybridoma supernatants were reactive on directly coated rMAp19 and directly coated MBL/MASP/MAp or H-ficolin/MASP/MAp complexes purified from human plasma, whereas they did not give appreciable signal on recombinant MASP-2 coated directly in wells. All final clones produced antibody of the IgM isotype, and also the MAp19-specific antibodies in the serum of the rat were almost exclusively IgM. The IgM antibodies could be readily purified on Protein L agarose and sustained biotinylation without appreciable loss of activity, but did not coat well, precluding their use as capture antibodies. The specificity of the anti-MAp19 antibodies was validated by performing Western blotting with purified MBL/MASP complex (Fig. 1C). As can be seen, the rat serum and all 6 final hybridomas were specific for MAp19, whereas the monoclonal antibody control (6G12) reacted with both MAp19 and MASP-2 (as well as some degradation fragments of MASP-2, which we have previously observed upon storage). There was no background staining on the control hybridoma strip.

The high similarity between the peptide immunogen and endogenous rat MAp19 along with the absence of class-switching indicated the induction of an autoimmune response. We examined whether the monoclonal antibodies were reactive with rat MAp19 by Western blotting. The purified antibodies and parental rat serum were tested on MBL/MASP and Ficolin/MASP complexes purified from human serum (control, Supplemental Fig. 1A) and rat serum (Supplemental Fig. 1B). Indeed, the purified antibodies reacted strongly with a band corresponding to the size of MAp19 of both human and rat origin.

3.2. Expression of mRNA encoding MAp19 and MASP-2 in human tissues

The levels of mRNA encoding MAp19 and MASP-2 were compared by qRT-PCR in a human tissue panel. β2-microglobulin mRNA levels were used for normalization. As previously reported (Stover et al., 2004; Seyfarth et al., 2006), MASP-2 mRNA was exclusively expressed in the liver (Fig. 2A). The site of highest relative expression level of MAp19 mRNA was also by far the liver, with very low expression seen in the thyroid and the kidney (Fig. 2B).

3.3. Tissue localization of MAp19 and MASP-2

In order to examine the tissue localization of MAp19 and MASP-2, one of the final clones (3B11) and a previously generated monoclonal anti-MASP-2 antibody (8B5) were applied to multi-block arrays of formalin-fixed and paraffin-embedded tissue sections (Fig. 3). The reactivity of the antibodies on formalin-fixed paraffin-embedded tissues and their specificity for MAp19 and MASP-2, respectively, was verified by control stainings of similarly prepared blocks of cells transfected with MAp19 or MASP-2, or mock transfected (Supplemental Fig. 2).

3F11 displayed strong staining of the cytoplasm of hepatocytes at the hexagonal edges of the lobules (Fig. 3A). A grainy staining of hepatocytes surrounding the central veins was also observed. However, this was deemed to be artificial staining of lipofuscin (not shown). Strong staining was also observed in

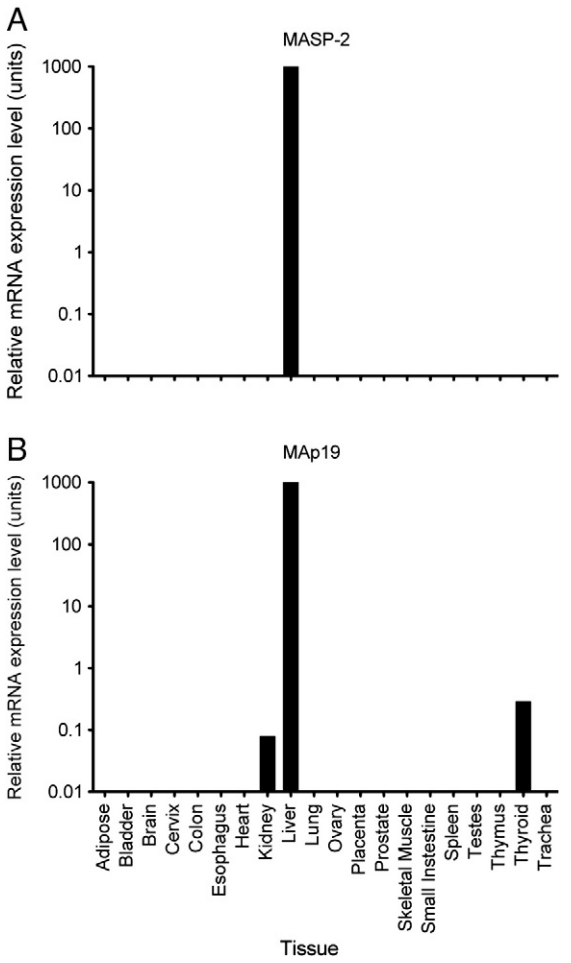

Fig. 2. MAp19 and MASP-2 mRNA in 20 human tissues. A) MASP-2 mRNA expression. B) MAp19 mRNA expression. Expression levels were calculated relative to β2-microglobulin levels and normalized to the liver.

alveolar macrophages, in polymorphonuclear cells, in very few cells in the thyroid, in exocrine cells of the stomach, and in prostate epithelium. In cerebellum there was weak staining of Purkinje cells, while there was a diffuse staining in the kidney.

The antibody specific for MASP-2 (8B5) stained hepatocytes in a speckled cytoplasmic pattern (Fig. 3B, see inset in liver panel for higher magnification), presumably reflecting exocytic vesicles in the cytoplasm. Alveolar macrophages were strongly stained, as were exocrine cells of the pancreas and few cells in the colon. Diffuse, but relatively strong staining was seen in the kidney.

3.4. Solid-phase assay for the measurement of MAp19

A solid-phase sandwich assay for MAp19 was constructed, in which the MASP-2 and MAp19 specific antibody, 6G12, was used for capture of MAp19 from serum and bound MAp19 was detected with biotinylated MAp19-specific antibody (4D12).

We produced recombinant MAp19 and purified this to homogeneity as assessed by SDS-PAGE and silver staining (Fig. 4A inset). In order to use the assay for quantification of MAp19, the concentration of this purified MAp19 was determined by spectrophotometry and quantitative amino acid analysis, and its titration curve was compared with that of a standard serum (Fig. 4A). As can be seen from the graph, the dilution curve of this preparation compared somewhat poorly with that of the standard serum. This was not due to a matrix effect, as diluting the recombinant material in MAp19/MASP-2-depleted serum gave a similar curve (Supplemental Fig. 3). Nonetheless, a credible quantitative estimation of the MAp19 level in serum could be obtained. Furthermore, addition of 13 ng, 7 ng or 3 ng recombinant MAp19 to serum diluted 1/20 (containing 6 ng endogenous MAp19) gave recoveries of rMAp19 of 84%, 102% and 103%, respectively. The total MAp19 measured in these samples was thus 88%, 101% and 101%, respectively.

The capacity and specificity of the assay was examined by adding two-fold dilutions of recombinant MAp19 or MASP-2 to one of the internal control sera (Fig. 4B). As seen, MASP-2 was not measured in the assay, and it did not start interfering with the assay until it reached grossly non-physiological levels above 1 μg added/ml (likely by competing for binding to the capture antibody, 6G12). This corresponds to MASP-2 levels of >20 μg/ml serum, which is 40 times higher than the reported mean of around 500 ng/ml (Møller-Kristensen et al., 2003). Conversely, a dose-response was seen with recombinant MAp19, until the assay began to reach saturation, above 1 μg added/ml.

The interassay coefficient of variation was determined based on the inclusion in each run of three internal controls: A) mean of 139 ng/ml, CV of 13% (n = 10); B) mean of 116 ng/ml, CV of 17% (n = 10); C) mean of 78 ng/ml, CV of 11% (n = 9).

3.5. MAp19 levels in Caucasians

The measurement of MAp19 in sera from 104 Danish blood donors, revealed a median MAp19 level of 217 ng/ml with a range from 26 to 675 ng/ml (Fig. 5A). For comparison, the mean level of MASP-2 is 534 ng/ml with a standard deviation of 213 ng/ml (Møller-Kristensen et al., 2003). While the levels of MASP-2 are log-normally distributed, the levels of MAp19 were neither normally nor log-normally distributed. We compared the levels measured in serum with those measured in plasma, in a set of 70 paired serum and plasma donor samples. Although slightly higher values were measured in plasma than serum (median 258 vs. 205 ng/ml) the values were highly correlated ($r^2 = 0.88$; Fig. 5B). MASP-2 levels were previously determined in the same samples (Ytting et al., 2007), allowing comparison of the MAp19 and MASP-2 levels. Based on Spearman nonparametric correlation analysis, there was no correlation between the levels of the two proteins (P = 0.81; Fig. 5C). We also did not see any correlation with serum concentrations of MBL, L-ficolin, M-ficolin, MASP-3 or MAp44, but observed a weak correlation with H-ficolin (rs = 0.23, P = 0.02; Fig. 5D).

3.6. MAp19 in urine

Considering the reported function of MAp19 as an inhibitor of calcium oxalate crystal formation (Kang et al., 1999) and the small size of MAp19, below the normal cut-off for glomerular filtration, even if dimeric, we decided to compare serum and urine levels (Fig. 6A and B). The mean MAp19 level was 204 ng/ml in the sera vs. 63 ng/ml in 24 h

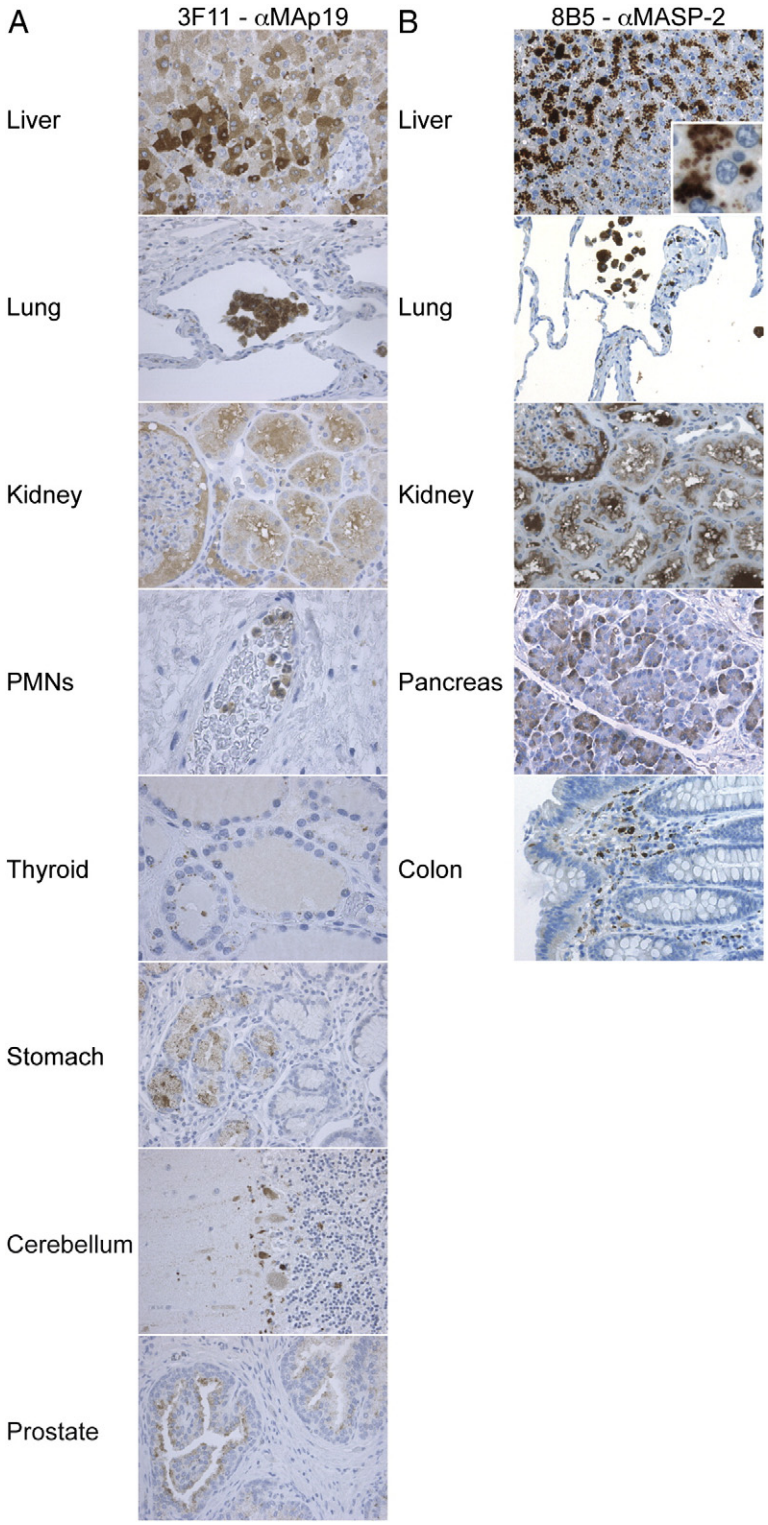

Fig. 3. Immunohistochemical analyses of MAp19 and MASP-2 tissue distribution. A) Immunohistochemical analysis of MAp19 expression in various tissues, using the clone 3F11. B) Immunohistochemical analysis of MASP-2 expression in various tissues, using monoclonal antibody 8B5. The inset in the 8B5 staining of liver is a further magnification to show cellular localization of staining.

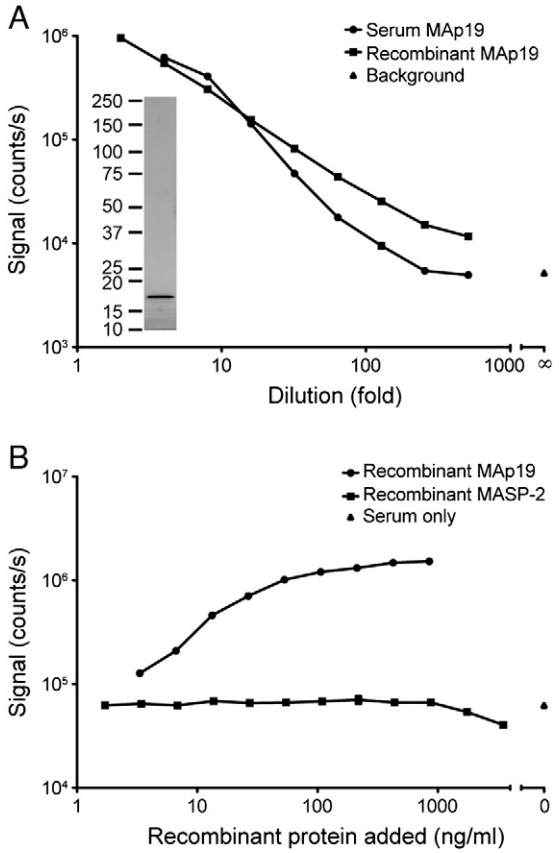

Fig. 4. The MAp19 assay. A) Comparison of titration curves for recombinant MAp19 and serum MAp19 in the MAp19 assay. Signals for recombinant MAp19 dilutions (-■-), serum MAp19 dilutions (-●-) and buffer background (♦) are given. Error bars indicating standard deviation of duplicates are within the size of the symbols used. The inset shows a silver stained SDS-PAGE of purified recombinant MAp19. B) Capacity and specificity test of the assay. Dilution curves of recombinant MAp19 (-■-) or MASP-2 (-●-) were added to serum diluted 20-fold. The abscissa indicates the amount of recombinant protein added per ml. Background for serum alone is indicated (♦).

urine of 5 male Danish donors. MASP-2 was measured in the same serum and urine samples yielding a median of 390 ng/ml serum, while urine levels were under the detection limit of the assay, i.e., below 1 ng/ml. There was no correlation between the serum and urine levels of the same individuals ($P = 0.52$, Spearman). The total amount of MAp19 excreted in 24 h was calculated based on the total urine volume of each individual (Fig. 6C), yielding a median of 127 μg. The total excretion was not correlated with the serum levels ($P = 0.45$, Spearman).

Many proteins excreted in urine are partially degraded. In order to examine whether the MAp19 measured in urine was indeed intact MAp19 and whether the measurements were reliable, we conducted Western blot analysis of the urine samples, using 4D12 (reducing conditions) and 1.3B7 (anti-MAp19/MASP-2, non-reducing conditions) (Supplemental Fig. 4). This indicated that indeed in one case, individual 4, MAp19 was partially degraded. As the blots developed with 4D12 and 1.3B7 were congruent, we can infer that the degradation fragment resulted from N-terminal cleavage. The presence of a degradation fragment of MAp19 was not dependent on storage, as the same picture was observed for samples stored frozen at −80 °C and samples stored at 4 °C for 10 months. Generally, the band intensities observed on WB seemed to correlate well with the levels measured in TRIFMA, i.e., individuals 1 and 4 presented the highest levels, followed by individual 5 and individuals 2 and 3.

3.7. Size distribution of MAp19 in human serum

We examined the size distribution of MAp19 in serum by GPC under native conditions or conditions dissociating MASPs and MAps from MBL and ficolins (Fig. 7). Under native conditions, in the presence of calcium, we saw a small peak at the elution volume of MBL and ficolin complexes, and two larger peaks at elution volumes corresponding to free MAp19 dimer and what might be a tetramer. Under dissociating conditions, i.e., high salt and EDTA, which dissociates MASPs and MAp19 from MBL and ficolins, the three peaks resolved into the two peaks at the size of the free dimer and putative tetramer. Surprisingly, this indicates that most of the MAp19 is not in complex with MBL or ficolins. Assuming that complexed and free dimer and tetramer MAp19 was measured with the same efficiency in the assay (carried out under dissociating conditions), the relative proportions of complex-bound and free MAp19 was estimated by integrating the area under the curve. This revealed that approximately 20% of MAp19 was found in complexes under native conditions, with ~80% being free.

3.8. MAp19 does not inhibit C4 deposition

We wished to examine the proposition that MAp19 competes with MASP-2 for binding to MBL (Iwaki et al., 2006). MBL was mixed with MASP-2 and various amounts of competitor, either MAp19 or MAp44, and then added to a mannan-coated surface. The wells were incubated at 37 °C with C4, allowing MASP-2 to cleave C4 to become deposited as C4b. Increasing amounts of MAp44 inhibited C4 deposition, whereas addition of MAp19 did not result in inhibition (Fig. 8). In order to control for possible differences in MBL complex binding to the surface or a possible inhibition of this by the competitors, we in parallel developed for bound MBL and found that binding of MBL was not affected (Supplemental Fig. 5).

4. Discussion

In a move toward creating a framework for understanding the biological function of the small product of alternative splicing of the primary *MASP2* transcript, we have addressed a major issue, namely the difficulty of raising antibody specific for MAp19. This issue was resolved and we provide a number of descriptive and functional characteristics of MAp19, which will hopefully further investigations into its function.

The generation of antibodies specific for MAp19 was hampered by the great similarity between MAp19 and MASP-2, with a unique sequence of only four amino acids distinguishing MAp19 from the first domains of MASP-2, together with the high degree of evolutionary conservation. The observed absence of isotype switching in the serum from the one responding rat might indicate a response related to the induction of auto-antibodies in the animal. Indeed, we found the anti-human MAp19 antibodies to cross-react with rat MAp19.

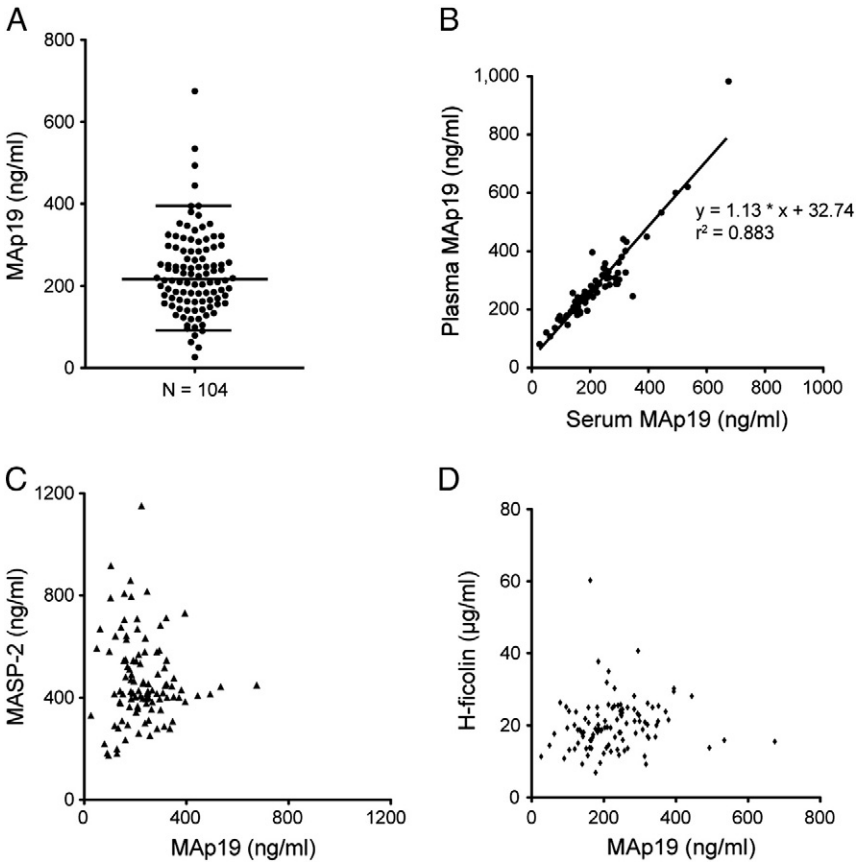

Fig. 5. Analysis of MAp19 levels. A) Distribution of MAp19 levels in serum of 104 Danish Caucasian blood donors. The broad horizontal bar represents the median, while the shorter bars indicate the 5th and 95th percentiles. B) Plot of levels of MAp19 measured in serum vs. plasma. C) Plot of MASP-2 levels vs. MAp19 levels. D) Plot of H-ficolin levels vs. MAp19 levels.

Protein localization may point toward function. We therefore used one of the generated antibodies, as well as a previously generated antibody toward MASP-2, in immunohistochemical analyses. We also quantified mRNA in various tissues to determine sites of synthesis. At the mRNA level, MAp19 expression was found predominantly in the liver, with significant but very low expression in kidney and thyroid tissue, while MASP-2 expression was completely restricted to liver. From the immunohistochemical analyses it further seemed that both MAp19 and MASP-2 are produced by hepatocytes. Very few cells were positive for MAp19 staining in the thyroid, and a diffuse staining was seen in the kidney. The latter may rather originate from the filtrate, especially considering the significant presence of MAp19 in urine. In addition to their sites of synthesis, MAp19 and MASP-2 staining was observed in a number of tissues, perhaps indicating secondary localization, or perhaps local expression (either not included, or below detection level, in the tissue RNA panels). Staining of alveolar macrophages warrants caution, as these phagocytes are notorious for high lipofuscin levels, and the same consideration applies to the long-lived Purkinje cells of the cerebellum. In conclusion, the liver is the major site of biosynthesis of both MAp19 and MASP-2.

The median level of MAp19 in serum of Danish blood donors was found to be 217 ng/ml. The serum level on a weight basis is thus lower than that of MASP-2 (mean: 534 ng/ml (Møller-Kristensen et al., 2003)), but this translates into a molar concentration of 11 nM and 7 nM for MAp19 (19.1 kDa mature) and MASP-2 (74.2 kDa mature), respectively. MAp19 and MASP-2 levels were not correlated. For comparison, the level of the other MBL/ficolin associated proteins are 1.7 µg/ml (41 nM) for MAp44 and 5.0 µg/ml (63 nM) for MASP-3 (Degn et al., 2010).

Median levels of 63 ng/ml in 24 h urine and 204 ng/ml in serum were found in 5 paired urine and serum samples. Somewhat surprisingly, the MAp19 levels in serum and urine were not correlated, and this was also not the case when looking at total urinary output. Intuitively, higher serum levels should result in higher urine output, assuming that MAp19 gets filtered in the glomeruli as suggested by its small size. One confounding factor may be the total level of MASPs/MAps compared to the total level of MBL/ficolins, since one could envision that MBL/ficolins may have a carrier function for MAp19, despite the apparently low affinity discussed below. For comparison median MASP-2 levels were 390 ng/ml serum and <1 ng/ml urine. This could be an effect both of the larger size of MASP-2 and of its strong association with MBL and ficolins.

MAp19 was originally identified as a protein co-purifying with MBL on affinity chromatography columns derivatized with MBL ligands (Thiel et al., 1997), and subsequent analyses have shown MAp19 to have a relatively high affinity for MBL (Kd of 13 nM). It was therefore surprising to find that only about 20% of MAp19 is associated with MBL or ficolins under native conditions. For comparison MASP-2 is found entirely in

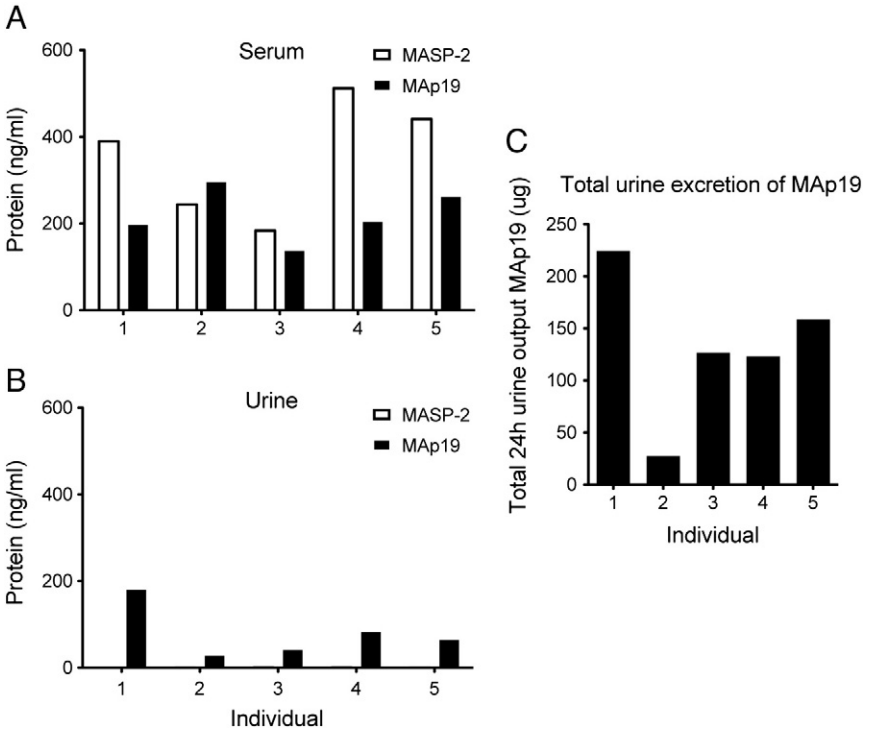

Fig. 6. MAp19 in urine. A) and B) Serum and 24 h urine levels, respectively, in 5 Danish males. C) Total 24 h urinary output of MAp19 in the same 5 individuals.

high molecular weight complexes under the same conditions (Møller-Kristensen et al., 2003).

A marked influence of the relatively small difference in affinity was also obvious when we found that contrary to MAp44, MAp19 showed no ability whatsoever to inhibit the lectin pathway of complement. This finding was surprising, since a previous report suggested that MAp19 acts as a competitive inhibitor of MASP-2 (Iwaki et al., 2006). However, the relative amounts of MAp19, MASP-2 and MBL used by Iwaki and colleagues were very far from the molecular stoichiometry *in vivo*, as the concentration of MAp19 was not known at that time. Thus, for their competition experiments, a constant amount of rMASP-2i (inactive mutant of MASP-2) of 0.5 μg and various amounts of rsMAP (rMAp19), from 0 to 20 μg, were incubated with 20 μl homozygous MASP-2/MAp19 −/− mouse serum. This corresponds to up to 1,000 μg/ml rsMAP competing with 25 μg rMASP-2i for binding to 0.84 μg MBL (7 μg MBL-A and 35 μg MBL-C per ml serum in B6 mice), disregarding the presence of ficolins-A and -B and MASP-1, -3, and MAp44. Considering that MAp19 is less than a third of the size of MASP-2, the molecular

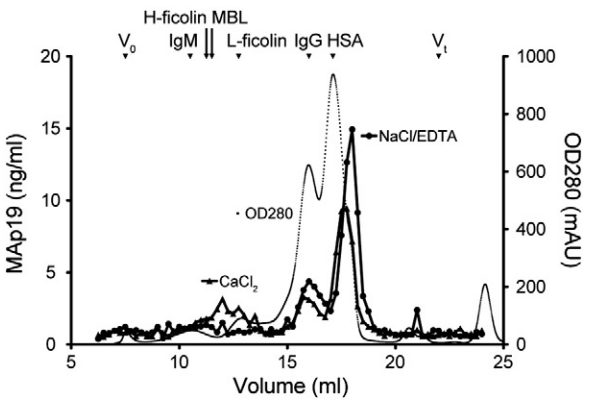

Fig. 7. Size distribution of MAp19 in human serum analyzed by gel permeation chromatography. Serum was run either at physiological conditions (-◆-, Tris-buffered saline with 5 mM $CaCl_2$) or at dissociating conditions (-●-, Tris buffer with 10 mM EDTA, 1 M NaCl) and fractions were measured in the MAp19 assay. The void volume, total volume and elution positions of protein markers are indicated. The total protein trace is also indicated (▪, OD280). Fraction volume is indicated on the x-axis (ml).

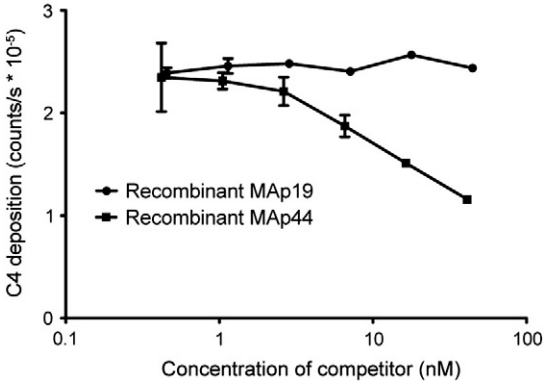

Fig. 8. The influence of MAp19 and MAp44 on C4 deposition. MBL was mixed with MASP-2 and MAp19 or MAp44, then added to mannan coated wells. Subsequently C4 was added and the wells were incubated at 37 °C. The amount of deposited C4b (in counts/s) is given as a function of the concentration of competitor, either rMAp44 (-■-) or rMAp19 (-●-). Error bars indicate standard deviation of duplicates. The experiment was performed three times with similar results, using slight differences in conditions and different batches of purified proteins.

stoichiometry is even more distorted. Whereas the experiments demonstrate that MAp19 can indeed compete with MASP-2, it appears that highly non-physiological conditions are required for such observations. At our conditions we see no evidence of such competition. Likewise for the C4 deposition, the lowest level shown is 100 ng rsMAP per 0.5 μl serum, i.e. 200 μg per 1.0 ml, which is close to 11 μM — a value which is 1,000 times, 3 orders of magnitude, higher than the physiological level determined here in man. We find it highly unlikely that the physiological levels should differ this significantly in mouse from that observed in man. Thus, while MAp19 concentrations far exceeding the physiological level may be able to compete with MASP-2, in our set-up we did not observe any competition. This may be explained by the more than 10-fold lower affinity of MAp19 for MBL, compared to that of the full-length MASP-2, as well as to MASP-1, MASP-3 and MAp44 counterparts (Degn et al., 2009; Degn et al., 2010). The lower affinity may in turn be explained by the absence of the CUB2 domain possessed by the full-length proteases and MAp44 (Thielens et al., 2001; Cseh et al., 2002).

The determination of these dissociation constants were based on Biacore analysis with curve fitting according to the Langmuir 1:1 interaction model, which are hardly applicable in this case of multivalent multimeric interacting molecules. Furthermore, the sensorgram for MASP-2 was hardly sloping, making it unsuitable for calculations. However, using a complementary approach, Chen and Wallis examined the importance of the N-terminal domains of MASPs for binding to MBL in an inhibition assay (Chen and Wallis, 2001). Rat MBP-A was immobilized on the solid-phase and competition of ^{35}S-labeled CUB-EGF-CUB binding was evaluated. Full-length MASP-1 and MASP-1 CUB-EGF-CUB yielded K_i's of 34 and 15 nM, respectively, while CUB-EGF yielded a K_i of 1810 nM. The same domain configurations for MASP-2 gave K_i's of 48, 22 and 454 nM, respectively. In both cases, this demonstrates the importance of the second CUB domain, in the case of MASP-1 increasing affinity 50-100-fold and for MASP-2 10-20-fold. The results for MASP-2 fragments can be extrapolated to MAp19.

Considering the relative levels of MAp19, MASP-2, MASP-1, MASP-3 and MAp44, and the fact that all the other molecules associate stronger with MBL and ficolin than MAp19, it appears unlikely that the biological role of MAp19 should be to act as a physiological inhibitor of complement.

In concordance with the above observations, the affinity purification procedure for rMAp19 using binding to MBL-derivatized Sepharose beads was inefficient compared to similar purification of recombinant MAp44, MASP-3 and MASP-2 using identical procedures (unpublished).

Our data leave open the question of the physiological role of MAp19. It remains a possibility that MAp19 has a function in calcium-homeostasis and regulation. The idea of a role in kidney function as suggested by (Kang et al., 1999) is appealing. Our literature review revealed a second paper pinpointing MAp19 in the kidney, but in relation to pathophysiology (Musante et al., 2002). Musante and colleagues identified "MASP-2" as one of only 6 protein factors that alter glomerular permeability in children with focal segmental glomerulosclerosis (FSGS). Upon closer inspection it is clear that what these authors refer to as "MASP-2" is really MAp19, based on the isoelectric point and size of the spot on 2D gel electrophoresis and the localization of mass spectrometry-identified peptide sequences to MAp19. Thongboonkerd and colleagues also identified "MASP-2" in normal human urine, and again this was actually MAp19, based on MW and pI (Thongboonkerd et al., 2002). Very recently, MAp19 (again referred to as MASP-2) was also found to be about 3-fold upregulated in urine of individuals undergoing cardiopulmonary bypass surgery (Aregger et al., 2010). Another unrelated role of MAp19 was suggested by a recent report that it interacts with the nucleocapsid protein of SARS-CoV (Liu et al., 2009).

The assay presented here allows the analysis of further human populations and possibly the identification of individuals deficient for MAp19, potentially furthering the elucidation of the role in humans.

In summary, we have produced monoclonal antibodies specific for MAp19, and using these, we have examined the tissue distribution of MAp19, we have set up a quantitative assay for MAp19, and we have determined the levels of MAp19 in serum and urine. In *in vitro* experiments using conditions reflecting the determined physiological concentrations of MASP-2 and MAp19, we find that MAp19 is unable to compete with MASP-2 for binding to MBL and hence did not impair complement activation. The physiological role of MAp19 remains unresolved.

Supplementary materials related to this article can be found online at doi:10.1016/j.jim.2011.08.006.

Acknowledgments

Nicole Thielens kindly provided human MAp19 cDNA in the pFastBac vector.

SED was supported by the Danish Graduate School of Immunology and the Lundbeck Foundation.

References

Aregger, F., Pilop, C., Uehlinger, D.E., Brunisholz, R., Carrel, T.P., Frey, F.J., Frey, B.M., 2010. Urinary proteomics before and after extracorporeal circulation in patients with and without acute kidney injury. J. Thorac. Cardiovasc. Surg. 139, 692.

Chen, C.B., Wallis, R., 2001. Stoichiometry of complexes between mannose-binding protein and its associated serine proteases. Defining functional units for complement activation. J. Biol. Chem. 276, 25894.

Cseh, S., Vera, L., Matsushita, M., Fujita, T., Arlaud, G.J., Thielens, N.M., 2002. Characterization of the interaction between L-ficolin/p35 and mannan-binding lectin-associated serine proteases-1 and −2. J. Immunol. 169, 5735.

Dahl, M.R., Thiel, S., Matsushita, M., Fujita, T., Willis, A.C., Christensen, T., Vorup-Jensen, T., Jensenius, J.C., 2001. MASP-3 and its association with distinct complexes of the mannan-binding lectin complement activation pathway. Immunity 15, 127.

Degn, S.E., Hansen, A.G., Steffensen, R., Jacobsen, C., Jensenius, J.C., Thiel, S., 2009. MAp44, a human protein associated with pattern recognition molecules of the complement system and regulating the lectin pathway of complement activation. J. Immunol. 183, 7371.

Degn, S.E., Jensen, L., Gál, P., Dobó, J., Holmvad, S.H., Jensenius, J.C., Thiel, S., 2010. Biological variations of MASP-3 and MAp44, two splice products of the MASP1 gene involved in regulation of the complement system. J. Immunol. Meth. 361, 37.

Degn, S.E., Andersen, S.H., Jensen, L., Thiel, S., Jensenius, J.C., 2011. Assay interference caused by antibodies reacting with rat kappa light-chain in human sera. J. Immunol. Methods 372, 204.

Dodds, A.W., 1993. Small-scale preparation of complement components C3 and C4. Meth. Enzymol. 223, 46.

Frederiksen, P.D., Thiel, S., Larsen, C.B., Jensenius, J.C., 2005. M-ficolin, an innate immune defence molecule, binds patterns of acetyl groups and activates complement. Scand. J. Immunol. 62, 462.

Gregory, L.A., Thielens, N.M., Matsushita, M., Sorensen, R., Arlaud, G.J., Fontecilla-Camps, J.C., Gaboriaud, C., 2004. The X-ray structure of human mannan-binding lectin-associated protein 19 (MAp19) and its interaction site with mannan-binding lectin and L-ficolin. J. Biol. Chem. 279, 29391.

Iwaki, D., Kanno, K., Takahashi, M., Endo, Y., Lynch, N.J., Schwaeble, W.J., Matsushita, M., Okabe, M., Fujita, T., 2006. Small mannose-binding lectin-associated protein plays a regulatory role in the lectin complement pathway. J. Immunol. 177, 8626.

Jensenius, J.C., Jensen, P.H., McGuire, K., Larsen, J.L., Thiel, S., 2003. Recombinant mannan-binding lectin (MBL) for therapy. Biochem. Soc. Trans. 31, 763.

Kang, I., Kim, J.I., Chang, S.G., Lee, S.J., Choi, S.L., Ha, J., Kim, S.S., 1999. Mannan-binding lectin (MBL)-associated plasma protein present in human urine inhibits calcium oxalate crystal growth. FEBS Lett. 462, 89.

Kearney, J.F., Radbruch, A., Liesegang, B., Rajewsky, K., 1979. A new mouse myeloma cell line that has lost immunoglobulin expression but permits the construction of antibody-secreting hybrid cell lines. J. Immunol. 123, 1548.

Kohler, G., Milstein, C., 1975. Continuous cultures of fused cells secreting antibody of predefined specificity. Nature 256, 495.

Krarup, A., Thiel, S., Hansen, A., Fujita, T., Jensenius, J.C., 2004. L-ficolin is a pattern recognition molecule specific for acetyl groups. J. Biol. Chem. 279, 47513.

Liu, J.L., Cao, C., Ma, Q.J., 2009. Study on interaction between SARS-CoV N and MAP19. Xi Bao Yu Fen Zi Mian Yi Xue Za Zhi 25, 777.

Matsushita, M., Thiel, S., Jensenius, J.C., Terai, I., Fujita, T., 2000. Proteolytic activities of two types of mannose-binding lectin-associated serine protease. J. Immunol. 165, 2637.

Møller-Kristensen, M., Jensenius, J.C., Jensen, L., Thielens, N., Rossi, V., Arlaud, G., Thiel, S., 2003. Levels of mannan-binding lectin-associated serine protease-2 in healthy individuals. J. Immunol. Meth. 282, 159.

Musante, L., Candiano, G., Bruschi, M., Zennaro, C., Carraro, M., Artero, M., Giuffrida, M.G., Conti, A., Santucci, A., Ghiggeri, G.M., 2002. Characterization of plasma factors that alter the permeability to albumin within isolated glomeruli. Proteomics 2, 197.

Nakajima, T., Ballou, C.E., 1974. Characterization of the carbohydrate fragments obtained from *Saccharomyces cerevisiae* mannan by alkaline degradation. J. Biol. Chem. 249, 7679.

Petersen, S.V., Thiel, S., Jensen, L., Steffensen, R., Jensenius, J.C., 2001. An assay for the mannan-binding lectin pathway of complement activation. J. Immunol. Meth. 257, 107.

Schwaeble, W., Dahl, M.R., Thiel, S., Stover, C., Jensenius, J.C., 2002. The mannan-binding lectin-associated serine proteases (MASPs) and MAp19: four components of the lectin pathway activation complex encoded by two genes. Immunobiology 205, 455.

Seyfarth, J., Garred, P., Madsen, H.O., 2006. Extra-hepatic transcription of the human mannose-binding lectin gene (mbl2) and the MBL-associated serine protease 1–3 genes. Mol. Immunol. 43, 962.

Stover, C.M., Thiel, S., Lynch, N.J., Schwaeble, W.J., 1999a. The rat and mouse homologues of MASP-2 and MAp19, components of the lectin activation pathway of complement. J. Immunol. 163, 6848.

Stover, C.M., Thiel, S., Thelen, M., Lynch, N.J., Vorup-Jensen, T., Jensenius, J.C., Schwaeble, W.J., 1999b. Two constituents of the initiation complex of the mannan-binding lectin activation pathway of complement are encoded by a single structural gene. J. Immunol. 162, 3481.

Stover, C.M., Lynch, N.J., Hanson, S.J., Windbichler, M., Gregory, S.G., Schwaeble, W.J., 2004. Organization of the MASP2 locus and its expression profile in mouse and rat. Mamm. Genome 15, 887.

Takahashi, M., Endo, Y., Fujita, T., Matsushita, M., 1999. A truncated form of mannose-binding lectin-associated serine protease (MASP)-2 expressed by alternative polyadenylation is a component of the lectin complement pathway. Int. Immunol. 11, 859.

Thiel, S., 2007. Complement activating soluble pattern recognition molecules with collagen-like regions, mannan-binding lectin, ficolins and associated proteins. Mol. Immunol. 44, 3875.

Thiel, S., Vorup-Jensen, T., Stover, C.M., Schwaeble, W., Laursen, S.B., Poulsen, K., Willis, A.C., Eggleton, P., Hansen, S., Holmskov, U., Reid, K.B., Jensenius, J.C., 1997. A second serine protease associated with mannan-binding lectin that activates complement. Nature 386, 506.

Thiel, S., Petersen, S.V., Vorup-Jensen, T., Matsushita, M., Fujita, T., Stover, C.M., Schwaeble, W.J., Jensenius, J.C., 2000. Interaction of C1q and mannan-binding lectin (MBL) with C1r, C1s, MBL-associated serine proteases 1 and 2, and the MBL-associated protein MAp19. J. Immunol. 165, 878.

Thielens, N.M., Cseh, S., Thiel, S., Vorup-Jensen, T., Rossi, V., Jensenius, J.C., Arlaud, G.J., 2001. Interaction properties of human mannan-binding lectin (MBL)-associated serine proteases-1 and −2, MBL-associated protein 19, and MBL. J. Immunol. 166, 5068.

Thongboonkerd, V., McLeish, K.R., Arthur, J.M., Klein, J.B., 2002. Proteomic analysis of normal human urinary proteins isolated by acetone precipitation or ultracentrifugation. Kidney Int. 62, 1461.

Ytting, H., Christensen, I.J., Thiel, S., Jensenius, J.C., Svendsen, M.N., Nielsen, L., Lottenburger, T., Nielsen, H.J., 2007. Biological variation in circulating levels of mannan-binding lectin (MBL) and MBL-associated serine protease-2 and the influence of age, gender and physical exercise. Scand. J. Immunol. 66, 458.